sustainability

MDPI

Article

Mechanical and Microstructure Properties of Biochar-Based Mortar: An Internal Curing Agent for PCC

Rayane Mrad and Ghassan Chehab *

Department of Civil and Environmental Engineering, American University of Beirut, Beirut 1107 2020, Lebanon; rnm18@aub.edu.lb

* Correspondence: gco6@aub.edu.lb

Received: 12 March 2019; Accepted: 20 April 2019; Published: 28 April 2019

Abstract: In pursuing sustainability targets, the construction industry has witnessed significant efforts exerted on exploring new alternatives for raw materials. Such initiatives aim to alleviate concerns of overexploitation of natural resources leading to their depletion. On a different note, the disposal of municipal solid waste (MSW) has also become a major concern in some countries, such as the case of Lebanon, where illegal dumping continues to take its toll on the environment. Pyrolysis has been introduced as a biomass decomposition process of MSW and is considered an environmentally friendly process that can mitigate open dumping. However, pyrolysis produces significant amounts of biochar as a byproduct that in turn needs to be disposed of or treated. This research aims to investigate the viability of using biochar as a sustainable alternative material to sand in cementitious mortar composites. A thorough microscale physicochemical characterization of the biochar is conducted prior to its inclusion in mortar. Then, its incorporation as a partial replacement of sand in mortar is assessed at the mesoscale level, based on performance indices that included compressive strength and microstructure properties. Analysis of the experimental results are used to provide guidelines and recommendations as to the effective incorporation of biochar fraction in cementitious mortar.

Keywords: biochar; mortar; sand; internal curing; absorption; pyrolysis

1. Introduction

The utilization of waste by-products in construction materials as replacement of raw materials constitutes an attractive alternative to disposal and an ecofriendly solution to the challenges concerning the shortage and exploitation of non-renewable natural resources in the world. Extensive research has been conducted to examine several waste by-products as a potential replacement of natural sand and fine aggregates for construction. To that end, crushed granite fines, fly ash, and limestone filler are some of the materials that have been found suitable [1,2]. Modolo et al. (2013) [3] explored the feasibility of using bottom bed ashes from combustion of forest biomass residues in bubbling fluidized bed combustors (BFBC) as a replacement of conventional sand in mortar formulations. It was concluded that its incorporation did not affect the mechanical properties of the mortars with respect to minimum required specifications [3]. Similarly, Andrade et al. (2009) and Torkittikul et al. (2017) suggested the use of bottom coal ash as a partial replacement of fine aggregates in concrete [4,5]. Results showed that as the incorporation volumes of coal bottom ash increased, the compressive strength remained the same as the control specimens, while the total shrinkage deformation as well as the density of mortar and concrete decreased noticeably, rendering it lightweight [4,5]. Bilir et al. (2015) studied the influence of fly ash as fine aggregate in mortar by studying its effect on workability, unit weight, compressive and flexural strength, modulus of elasticity, and stress–strain behavior [6]. The study reported a decrease

in compressive strength, estimated at 73.1%, and an increase in ductility, represented by the delay in crack formation due to drying shrinkage, in the presence of 100% fly ash volumes [6].

1.1. Literature Review/Background

1.1.1. Production Process and Physicochemical Properties of Biochar

Biochar is one of the waste by-products that has been recently studied for its possible use in cementitious and asphaltic composites in infrastructure applications [7]. It is a carbon-rich solid residue resulting from the thermochemical conversion of biomass or municipal solid waste (MSW) in an oxygen limited environment, an environmentally friendly and energy-efficient waste treatment process known as pyrolysis [8].

In general, energy obtained from pyrolysis can be cleaner than that from conventional MSW incineration as it produces lower amounts of sulfur and nitrogen oxides [9]. MSW is first pretreated by source collection separation, including sorting and shredding, and then heated externally with combustion gas from pyrolysis, all while being mixed in the reactor. Throughout this process, the physical and chemical state of biomass undergoes simultaneous change, during which the color, weight, size, and mechanical strength change, and syngas, bio-oil, and char form [10]. At temperatures around 350 °C, the feedstock disintegrates by up to 80% in weight and the remaining feedstock forms char, known as biochar.

Biochar is known for its high carbon (C) content, existing in the form of aromatic compounds, characterized by rings of six carbon atoms linked together without oxygen or hydrogen [11]. These compounds are arranged in an irregular manner and in complex forms. The physical and chemical composition of biochar depends largely on the heating rate, combustion temperature, and the particle size of the feedstock [12,13]. Its composition and particle size can closely resemble that of its feedstock. For example, elements found in biochar from biomass can include calcium, copper, iron, potassium, magnesium, nickel, phosphorous, sulfur, zinc, and silica [12]. The higher the temperature and residence time, the less carbon, oxygen, and hydrogen remain in the solid residue [12]. The density of Biochar is low ranging between 0.2 and 0.5 g/cm^3 and is also dependent on the feedstock and process. Biochar with low carbon contents has higher densities due to excess minerals. As for biochar particle density, it is usually in the range of 1.5 to 1.7 g/cm^3 and increases with pyrolysis temperature [12].

In addition, the escape of volatiles and organic matters from the feedstock during pyrolysis induces pores of different sizes and ranges in the biochar, and gives it a honeycomb-like pore structure, making of it a highly porous material that can absorb and sustain an appreciable amount of water in its pores that can be used for internal curing in mortar, as is the case with lightweight aggregate (LWA) applications. It is also known for its capability of absorbing and sequestering carbon, greenhouse gases, and nutrients for a long period of time, favoring its application in soils.

The porosity of biochar can be categorized in three different scales: Micropores, mesopores, and macropores and each has a different range of pore size and affects the behavior differently. The larger the pores, the easier the water can penetrate the particles [12]. Considering these properties, biochar is being introduced in construction material such as concrete, mortar, and even asphalt binders as an internal curing agent and a potential reducer of atmospheric carbon [13,14].

1.1.2. Internal Curing in Cementitious Composites

The high porosity of biochar qualifies it to be considered as an internal curing agent in cementitious materials [13,14]. Internal curing consists of supplying water to the hydrating Portland cement paste from the onset of mixing to increase the degree of hydration when needed. This is achieved by introducing a well-dispersed water saturated material, acting as water-filled reservoirs in Portland cement concrete [15,16]. It differs from conventional curing where water is provided to the surfaces of the concrete after placement, which allows water to penetrate only a few millimeters beyond the surface [17]. Effectiveness of internal curing is a function of various factors, the importance of

which are the water absorption capacity of the material being introduced in the concrete (i.e., the volume of water available for internal curing), the ability of the material to release the water to the surrounding paste when needed, and the effective distribution of the material particles so that they are well dispersed and water can readily travel to all the paste sections [18]. Therefore, the selection of the appropriate material is a governing factor that could either improve or impede the process of internal curing and must be investigated by means of physical and chemical characterization. Aggregates with high porosity can maintain humid conditions in mixtures and compensate the loss of water due to evaporation and provide continuous water supply, thus preventing the cement from undergoing substantial self-desiccation [19].

Internal curing has a significant effect on concrete and mortar in terms of strength, shrinkage, cracking, and durability [20], and its effectiveness has been quantitatively proven in many studies [19–21]. Benefits of internal curing has been shown to include increased compressive or flexural strength of mortar, especially at later stages [22], in addition to mitigating or eliminating micro cracking in low water/binder ratio mixes, due to the deformation of the cement paste [23]. The primary function of the additional water provided by the pores of these materials is to offset the empty pore spaces of the matrix created during the chemical shrinkage reactions at the early stages of hydration [24], as well as promoting pozzolanic reactions at the interface of the aggregates and cement paste, which further contributes to the strengthening of their interfacial bond.

The effect of aggregate particles on the microstructure of concrete and mortar continues to be of major interest for researchers, since it controls the mechanical strength and durability [25]. The strength of the bond between the aggregates and the cement paste matrix, a zone called the interfacial transition zone (ITZ), is affected gravely by the morphology of the aggregates, including the size, texture, shape, roughness, and porosity of the aggregates [26]. The ITZ, in turn, has a significant effect on the mechanical properties of the mortar and concrete [27]. Many studies have been done to investigate the effect of aggregate properties, mainly absorption and release of water from aggregates, on the ITZ formation [25,28]. It was found that aggregates with high porosity and a subsequently higher tendency to absorb and release water increase the hydration degree of the paste around the aggregate. This would reduce the wall effect that exists at the aggregate–cement interface and results in a more continuous and uniform microstructure [25–28].

Beneficial uses of biochar span a variety of applications related to civil infrastructure, including concrete pavements. Recently, state highway agencies have been proactive in their efforts to upscale the research on internal curing in Portland cement concrete from laboratory level to field applications. Such applications include but are not limited to railway transit yards, bridge decks, and concrete pavements [18–21].

1.2. Research Objectives and Scope of Work

In this research, biochar from the pyrolysis of MSW is investigated as a potential replacement for sand in Portland cement mortar. This not only provides a solution for the waste disposal problems, but also saves on the use of non-renewable natural resources globally and offers an environmentally friendly source of construction material constituents. With its porous cellular structure able to absorb and maintain water, biochar is investigated for possibly serving as an internal curing agent in mortar by pre-soaking in water prior to mixing. Its effect on mortar properties is quantified by reported measurements of the compressive strength and the mechanical interlocking between the biochar particles and the cement at the interfacial transition zone on the microstructural level.

The scope of work consists of a series of laboratory investigations and testing on biochar, and on cement mortar with varying biochar contents. The experimental work is divided into two phases: (1) The experimental analysis at the microscale level, where the physical and chemical properties of biochar particles are characterized, and (2) at the mesoscale level, where the contribution of biochar in cementitious mortar composites is assessed, based on the mechanical and microstructural properties of the mortar.

2. Materials and Methods

2.1. Constituent Materials

Type I Portland cement obtained from LafargeHolcim plant in Chekka, Lebanon, was used throughout this study. Natural sand was obtained from a local quarry in Beqaa, Lebanon, and used for the production of all mortar mixes. The biochar was produced from the slow pyrolysis of municipal solid waste (MSW), treated at temperatures ranging from 300 to 400 °C, at the Green Eco-tech plant located in Zrarieh, Lebanon. The biochar was obtained in two size categories: Coarse aggregates and powder (filler).

Figure 1 presents the particle size distribution (PSD) of biochar and sand. The gradations are deemed acceptable for use in Portland cement mortar and concrete (PCC) since the produced mortar complies with strength requirements as per ASTM C270. Biochar has a coarser gradation than sand, with a fineness modulus of 3.45, compared to 1.71 for sand. Biochar replacement of sand was done on a sieve basis for selected sieve numbers 30, 50, 100, and 200. The specific gravity of biochar and sand was 0.668 g/cm^3 and 1.462 g/cm^3, respectively.

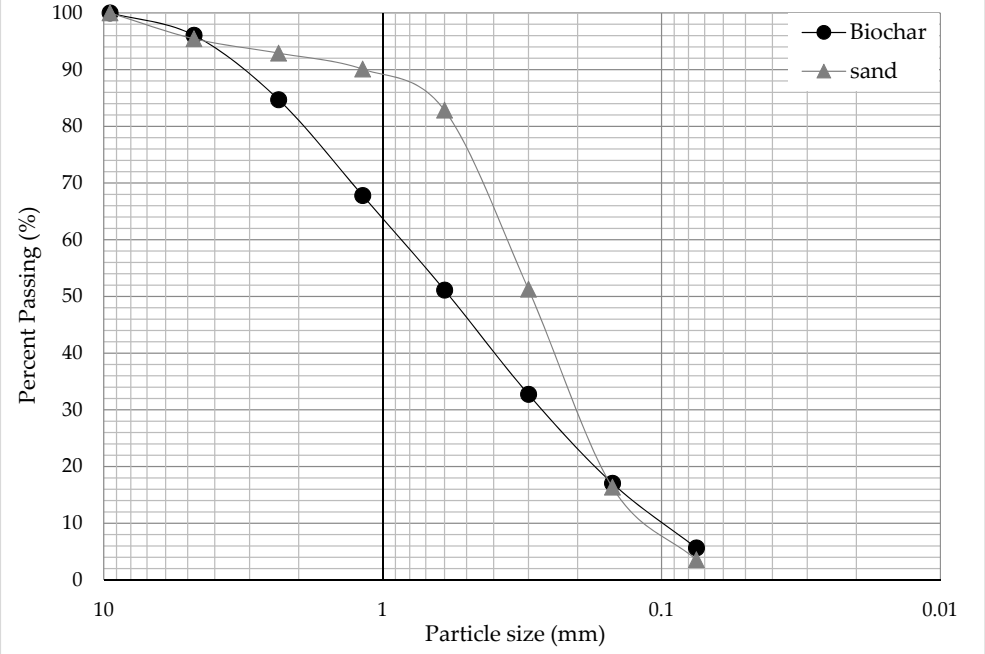

Figure 1. Particle size distribution of biochar and sand.

2.2. Water Absorption and Desorption Behavior of Biochar

The water absorption profile and saturation point of biochar were determined following the ASTM C128 test method. Figure 2 presents the water absorption capacity of biochar, which is approximately 60% after 48 h of soaking.

Desorption is the rate at which the aggregates lose their absorbed water during drying conditions, a rate critical for achieving an effective internal curing process. For this study, desorption isotherms of pre-saturated biochar particles were measured at relative humidity (RH) conditions, ranging from 95 to 0%. Biochar samples were oven-dried for 24 h, saturated in distilled water for 48 h, and left to reach their saturated surface dry conditions (SSD) prior to testing. The samples were then placed in controlled climatic chambers of different RH for 72 h until stable mass was reached, and mass measurements were recorded. Figures 3 and 4 show the water desorption behavior of biochar measured in the lab and from literature review, respectively.

The first point at 100% RH indicates the water absorption. It is observed that the biochar released only 10% and 20% of its absorbed water at 95% and 75% relative humidity, respectively (Figure 3). A desirable desorption behavior for efficient internal curing consists of the release of a significant amount of the absorbed water when the concrete is still maturing (i.e., at high relative humidity, typically between 93% and 95%) [29]. As such, the water desorption of biochar is considered lower than other conventional internal curing agents, such as lightweight aggregates); however, this only makes it a less efficient agent and does not eliminate its internal curing potential.

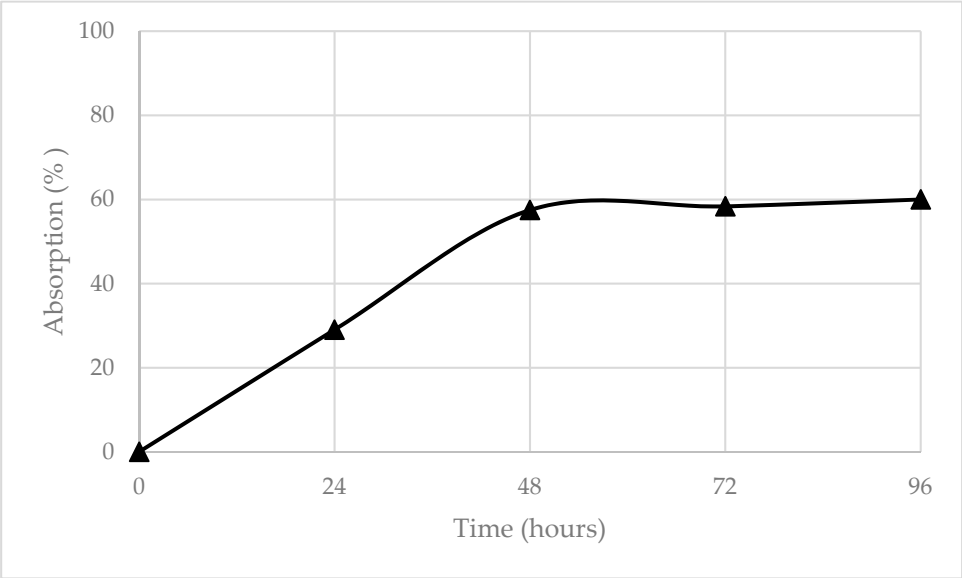

Figure 2. Time-dependent water absorption profile of biochar.

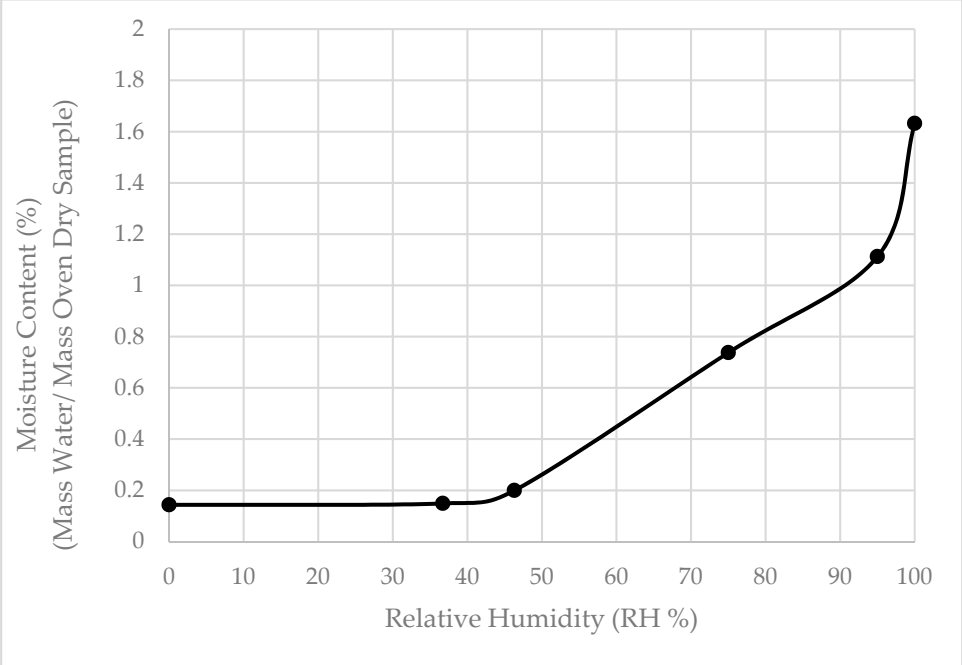

Figure 3. Water desorption profile of biochar at different relative humidity levels (RH %), starting from saturated surface dry conditions.

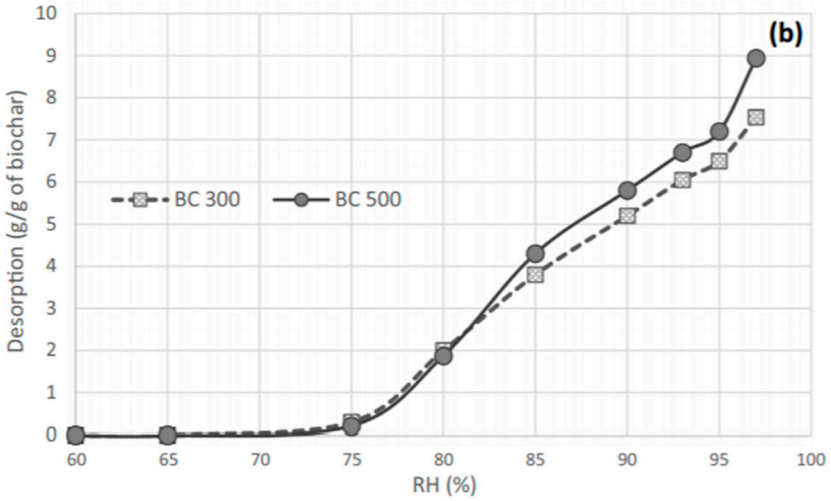

Figure 4. Water release (g/g of saturated char) from biochar particles, produced at 300 °C and 500 °C at different relative humidity [30].

2.3. Mineralogical Composition, Morphology, and Elemental Composition of Biochar

The biochar's particle size, shape, texture, and composition directly impact the nature of the aggregate–cement paste interface, a critical factor affecting strength and durability of cementitious composites. Several biochar samples were taken from four randomly selected batches of the plant to capture any variability that might exist among produced batches. The samples were finely ground and homogenized for the characterization of their crystallographic structure and mineralogical composition, using the X-ray diffraction (XRD) test. The XRD patterns of the materials are shown in Figure 5. A qualitative assessment of the crystallinity of the samples can be obtained from the intensity of the narrow reflections, as compared to the broad band around 22° and 30° (2θ). The graph shows sharp diffraction peaks indicating an intense pattern of calcite (CaCO3), which represents the bulk composition of biochar.

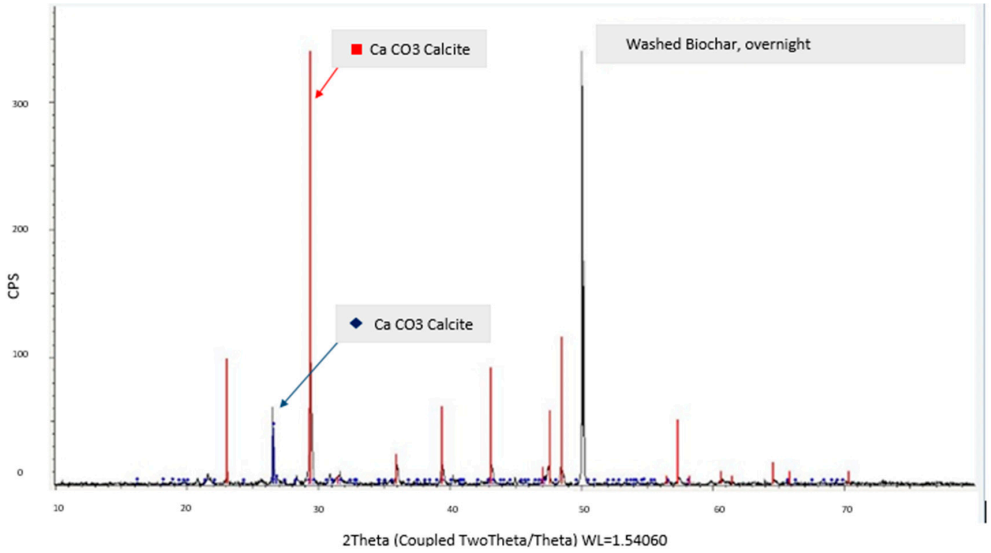

Figure 5. Mineralogical composition of biochar samples: Intensity (counts/seconds (CPS)) vs. 2θ (degrees).

Figure 6a,d shows scanning electron microscopy (SEM) images of biochar and sand particles under the microscope, respectively, for the different sizes used in the PCC mix. Magnified images in Figure 6b,c reveal the roundness and smooth surface texture of sand particles with the existence of few micropores, whereas Figure 6e–f reveals the irregular and elongated shape of biochar particles.

Additionally, the biochar particles are characterized with a rough and microporous cellular structure consisting of interconnected fibers. This is indicative of high water absorption and retention capacity and is probably inherited from the biological capillary structure of the feedstock.

The elemental composition of the biochar was determined via energy-dispersive X-ray spectroscopy (EDX), fitted together with the scanning electron microscope. Random spectrum points on SEM images were selected and analyzed. The biochar was found to contain about 60% carbon. The other major elements are oxygen at 27% and calcium (Ca) at 7%, in addition to traces of silica (Si), magnesium (Mg), aluminum (Al), sodium (Na), and chloride (Cl). In addition, testing for commonly existing heavy metals from MSW in biochar samples, such as Pb, Cd, Cu, Ni, Zn, and Cr, showed insignificant concentrations compared to the maximum allowed threshold for national primary drinking water regulations, as stated by the EPA [31].

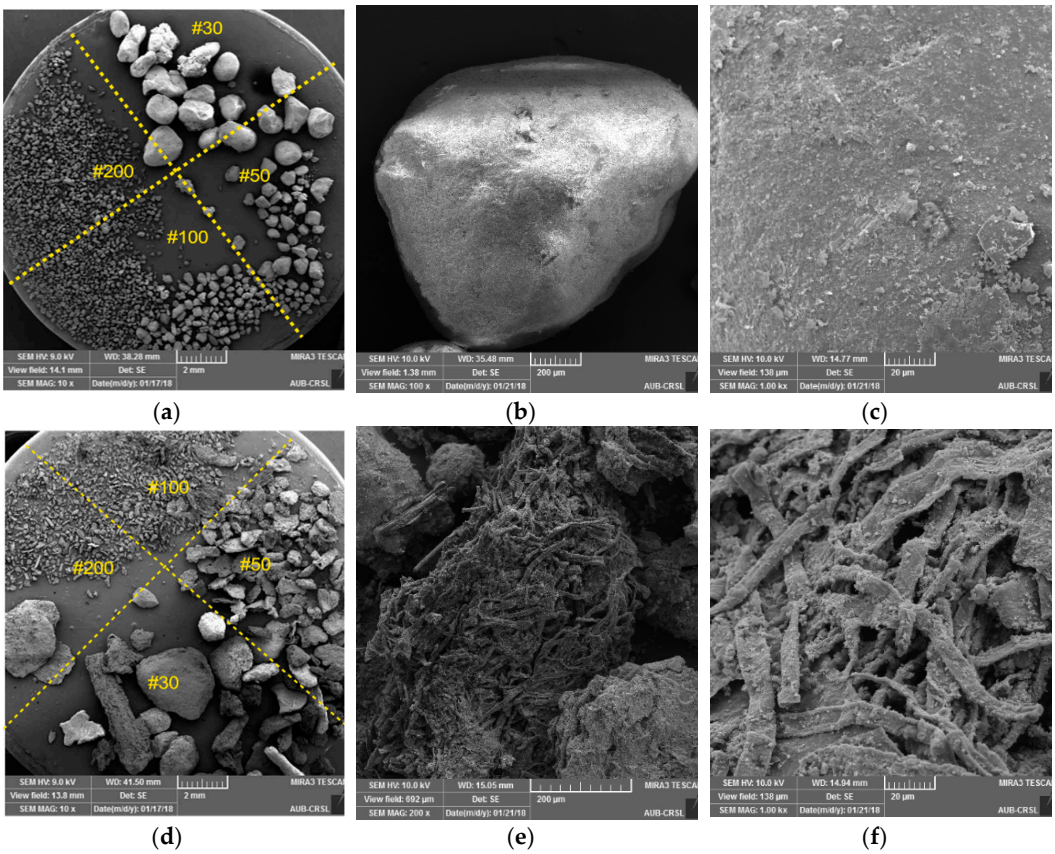

Figure 6. Scanning electron microscopy images at different magnifications: (**a**–**c**) Of sand; (**d**–**f**) of biochar.

2.4. Mortar Mix Design and Fabrication

To determine the effect of biochar on the performance of the different components of hardened mortar, six different mortar mixtures were prepared with an effective w/c ratio of 0.43 and a binder to fine aggregate mix ratio of 1:3. This included a plain mortar mixture designated as 0.0% and five other mortar mixtures with varying amounts of water-saturated biochar aggregates as a replacement of sand, as shown in Table 1. The biochar replacement of sand was done on a sieve basis for sieve numbers 30, 50, 100, and 200.

The mixing of mortar was carried out using a mechanical mixer, as per ASTM C305-14. The biochar was oven-dried, air cooled, and then submerged in water for 48 h prior to mixing. The sand was oven-dried and cooled for 24 h before mixing. After mixing, the mortar was cast in 50-mm metal molds and placed in a closed room to set and harden at 76 ± 2% relative humidity and 23 ± 20 °C for 24 h (prevalent room temperature).

To determine the effect of internal curing provided by the biochar on the compressive strength of mortars, two curing regimes were adopted: Air curing and water curing. For water curing conditions, specimens were immersed in water in a curing room, removed, and left to dry at room temperature, until one day before testing. For air curing conditions, two boundary conditions were tested for:

- Sealed conditions: Samples were sealed under vacuum, in puncture-resistant polymer bags to experience internal drying only (Figure 7d). The sealed system prevents loss or gain of moisture present in the surrounding environment and thus increases the hydration reactions with the existing mixing water content [16];
- Unsealed conditions: Samples were exposed to room temperature and constant relative humidity of 76% and allowed to undergo both internal and external drying (Figure 7b).

At first, only mixes with 10%, 25%, and 45% biochar replacement were fabricated and tested for compressive strength under both curing conditions. This was done to determine the maximum biochar contents that can be incorporated in mortar and their effect on the mechanical performance. However, after analyzing the results that depicted low compressive strength values, lower percentages of biochar were targeted, mainly between 0 and 15%, and for air-curing conditions only.

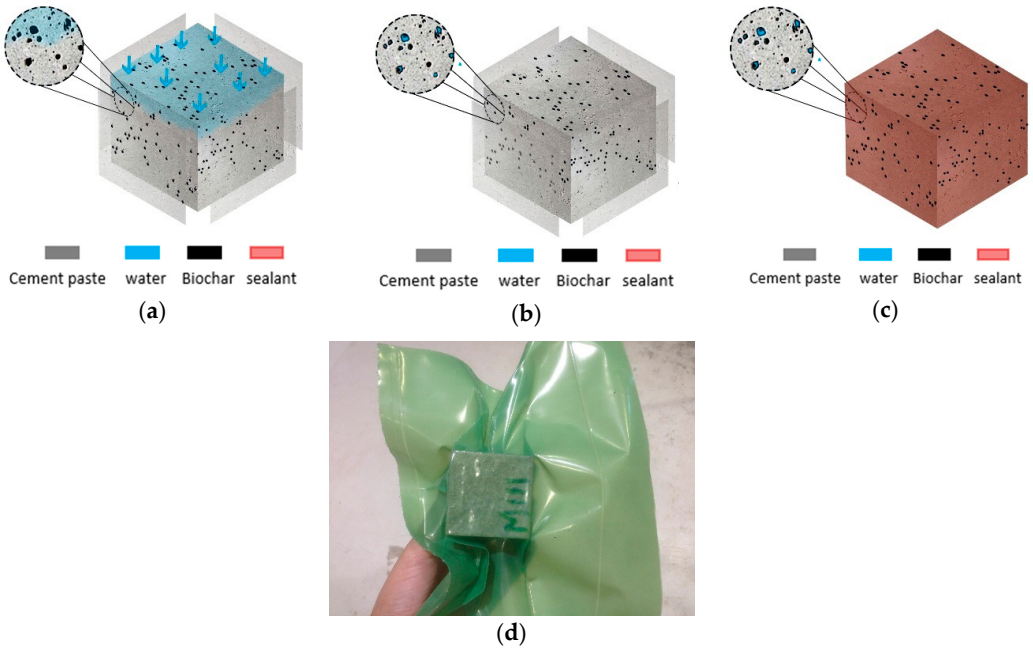

Figure 7. Different curing conditions: (**a**) Unsealed and water-cured; (**b**) unsealed and air-cured; (**c**) sealed; (**d**) 50-mm cube sealed under vacuum, using polymer bag.

Table 1. Mix Designs for Mortar.

Mix Id	Biochar (%)	Cement (g)	Sand (g)	Biochar (g)	W/C	Curing Conditions
M0	0.0	271.0	792.0	0.0	0.43	Air and Water Cured
M1	5.0	271.0	752.4	39.6	0.43	Air Cured Only
M2	10.0	271.0	712.8	79.2	0.43	Air and Water Cured
M3	15.0	271.0	673.2	118.8	0.43	Air Cured Only
M4	25.0	271.0	594.0	198.0	0.43	Air and Water Cured
M5	45.0	271.0	435.6	356.4	0.43	Air and Water Cured

2.5. Compressive Strength

A total of 132 mortar cubes (50 mm) were produced for all mixes: M0, M1, M2, M3, M4, and M5, following ASTM C109. First, the strength of mortar cubes was determined for three replicates for each mix at 7, 14, and 28 age days, except for mixes 1 and 3.

2.6. Interfacial Transition Zone (ITZ) Using SEM

The characterization of the biochar–cement and sand–cement interfaces was qualitatively assessed and investigated, using the SEM. Prismatic specimens of size 285 × 25 × 25 mm were produced for this purpose. The specimens were sectioned into 50 × 25 mm-thin slices and then impregnated with a low viscosity epoxy in a vacuum desiccator. Following epoxy impregnation, specimens were polished, and scanning electron microscopy (SEM) images were obtained and analyzed, using the X-ray EDS mapping tool. Images were acquired randomly around aggregates at several magnifications of 400×, 600×, 800×, and 1000×.

3. Results and Discussion

3.1. Compressive Strength

3.1.1. Effect of Biochar Replacement on the Compressive Strength of Mortar Cubes

Figure 8 presents the compressive strength of mortar cubes for plain mortar mixes (M0) and mixes containing 10% (M2), 25% (M4), and 45% (M5) of biochar under both curing conditions, dry and soaked. In general, the compressive strength of mortar decreased with increasing replacement percentage of sand with biochar under both curing conditions.

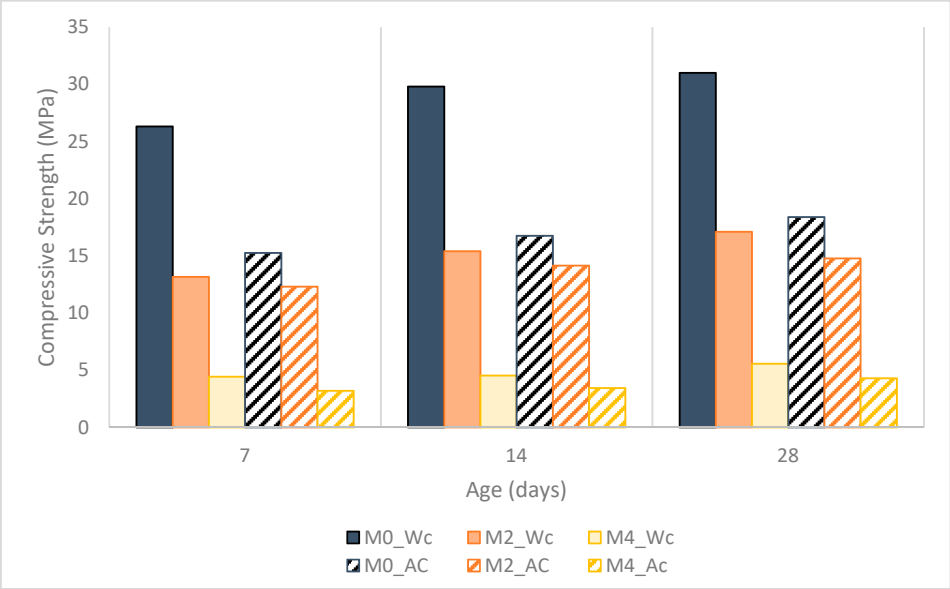

Figure 8. Compressive strength of mortar cubes for mixes 0, 2, 4, and 5 under water curing (Wc) and air curing (Ac) conditions at 7, 14, and 28 days.

For samples under air curing conditions, M4 and M5 exhibited significant drops in strength, estimated at 77% and 93%, respectively, after 28 days, as compared to M0. As for M2, the drop in strength was estimated at 19%. However, when cured in water, the same mixes showed a higher drop in strength, estimated at 82%, 97%, and 50%, respectively, after 28 days.

The reason behind the higher drop in compressive strength for specimens cured in water can be attributed to the porous nature of biochar and its high water absorption capacity. With this physical

property, the biochar tends to absorb excessive quantities of water, to an extent that becomes detrimental to the mortar properties.

Conversely, under air curing conditions, the drop in strength could be explained by the fact that the biochar particles were only partially saturated (soaked for 24 h only) prior to their inclusion in the mix, which allowed them to absorb and retain part of the mixing water and thus lower the designed w/c ratio. Since biochar contents beyond that were detrimental to the compressive strength of mortars, only mixes M1 (5%), M2 (10%), and M3 (15%) were considered for the remainder of the experimental program.

3.1.2. Effect of Internal Curing on the Compressive Strength of Mortar Cubes

The effect of internal curing was evident under dry conditions (i.e., air cured and sealed conditions). Under air curing conditions, the compressive strength of M0 (control mortar without biochar) was 40.7% less than that cured in water. Interestingly, for mortar mixes with 10% and 25% biochar, the loss in compressive strength for dry samples was less than that observed from the control (M0): To 15.2% and 22.8% respectively, compared to 40.7%. As expected, a gain in strength of 48.2% was observed for the biochar volume fraction of 45% (Figures 7 and 8). More analyses and conclusions can be made from Figures 8 and 9:

- Increase in strength with increasing number of days for all mixes and curing conditions, which is expected;
- Compressive strength decreases slightly with increase of biochar content up to 10%. After that, the drop becomes significant;
- Compressive strength loss between control mortar and mortar with biochar is more significant for water cured samples;
- The development and values of compressive strength for 5% and 10% biochar replacement are almost identical, suggesting an acceptable upper limit of 10% biochar. The strength drops significantly after that, as witnessed for 15% biochar replacement samples.

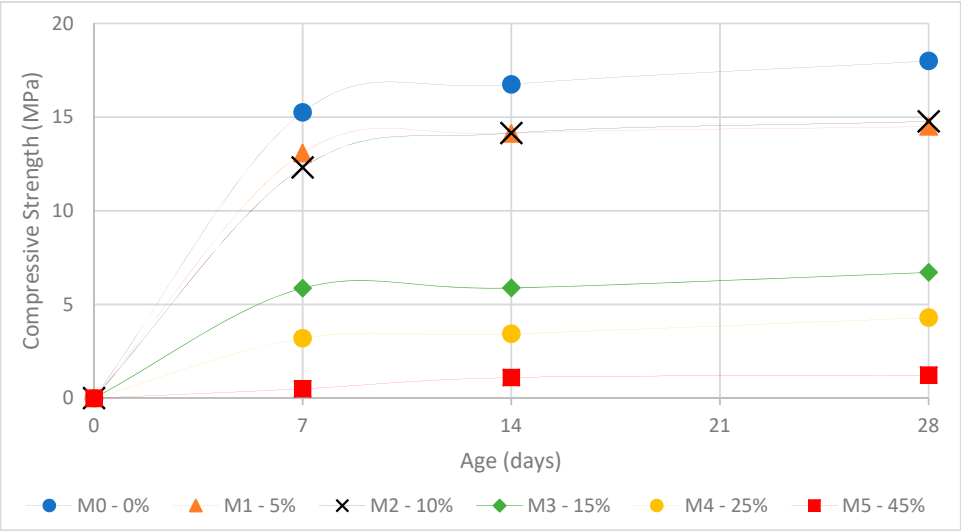

Figure 9. Compressive strength of mortar cubes for all mixes at 7, 14, and 28 days under air curing conditions.

For specimens sealed under vacuum, a minimal drop in strength is observed up to replacement rates of 10%; a significant drop ensues with additional replacement after that. At the age of 28 days, samples sealed under vacuum showed a higher compressive strength than the ones exposed to drying conditions and this remained true for all biochar replacement rates (Figure 10). However, this increase

in strength augmented from 17.5% for M0 successively to 22%, 27.7%, and 62.9% for M1, M2, and M3 (5%, 10%, and 15% biochar replacement, respectively). Under sealed conditions, the sample undergoes only self-desiccation and does not lose or gain water from the surrounding environment, due to surrounding sealed boundary conditions (i.e., sealed in polymer bags). Thus, the sole factor contributing to the strength upsurge would be the increase in the hydration reactions, due to the water supplied by the biochar particles to the surrounding cement paste. This means that the internal water made available for internal curing maintained a desired internal relative humidity level and resulted in a denser microstructure in the absence of adequate curing conditions.

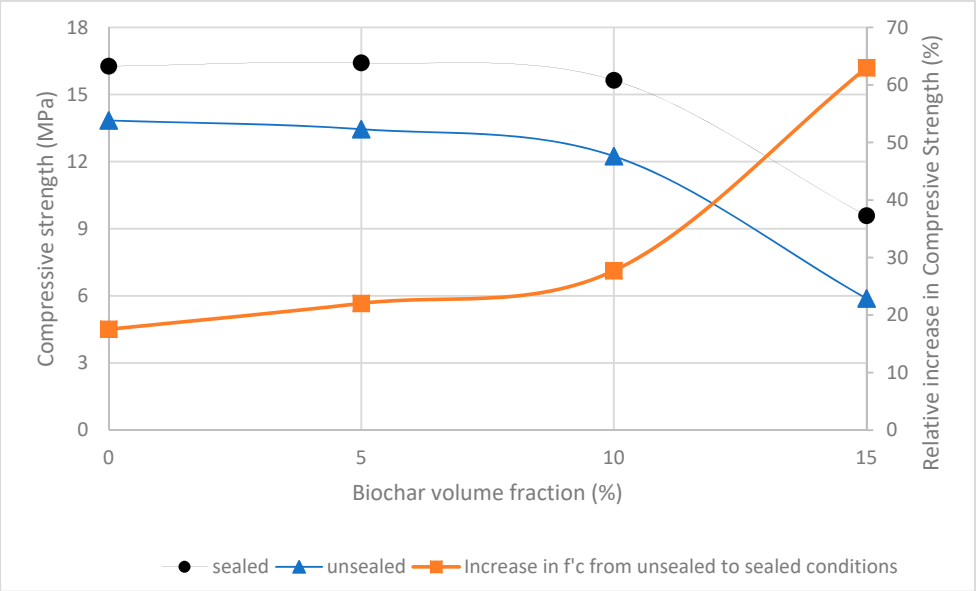

Figure 10. Compressive strength of mortar mixes containing different replacement rates of biochar under sealed and unsealed conditions at the age of 28 days.

3.2. *Interfacial Transition Zone (ITZ)*

SEM images and X-ray element mapping were done to identify and assess the ITZ at the outer rim of the biochar particles and compare it to the ITZ at the sand–cement paste interface. The release of water from the biochar is expected to strengthen the interfacial bond between the biochar particles and the bulk cement paste and result in a denser, progressive, and more uniform zone.

Many studies have examined the microstructure of the hardened mortar with and without internal curing and it was found that internal curing can improve the concrete durability by inhibiting the formation of the percolated pathways and densifying the interfacial transition zone (ITZ) between the porous aggregates and cement paste [15,16,19,32,33]. Lam (2005) studied the effect of saturated LWA and superabsorbent polymers on the microstructure of hardened concrete specimens, using scanning electron microscopy (SEM), and determined that a mechanical interlocking between the paste and the pores at the surface of the aggregates strengthened the bond at the ITZ and made it superior to that of normal-weight aggregate concrete [23]. Other researchers established the idea that porous aggregates with a rough surface texture allow the penetration of the cement paste and hydration products, indicated by the presence of calcium and sulfur elements, into the surface pores and thus bind the aggregates and the matrix together, resulting in good strength development and low permeability [23,34,35]. This strong bonding thus renders it difficult to distinguish the separation between the LWA and the cement paste [23]. An indirect proof of the strong mechanical interlock between the LWA and cement paste is the propagation of the cracks through the aggregates instead of along their rim, as would be the case with normal weight aggregates [20].

In the SEM images, the hydrated phases and sand aggregates appear as grey, while porosity appears near black. The biochar particles appear as a porous system with pores that are very close, yet not connected to each other. In Figure 11a, a sand aggregate next to the cement matrix is spotted and a continuous junction black line at the outer rim of the sand particle appears as the interfacial transition zone. A microcrack probing out from the ITZ perpendicularly to the sand aggregate is also detectable. Zooming in to a magnification of 6000×, a complete detachment of the cement paste from the sand particle is observed and deposits of crystal structures of hydration products are clear in Figure 11b. Clustered sand aggregates surrounded by a cement matrix are shown in Figure 12a. X-ray mapping analysis shows a high concentration of calcium around the aggregates in the form of a belt while silica clearly outlines the sand aggregates. These elements can be attributed to the presence of calcium hydroxide along the ITZ.

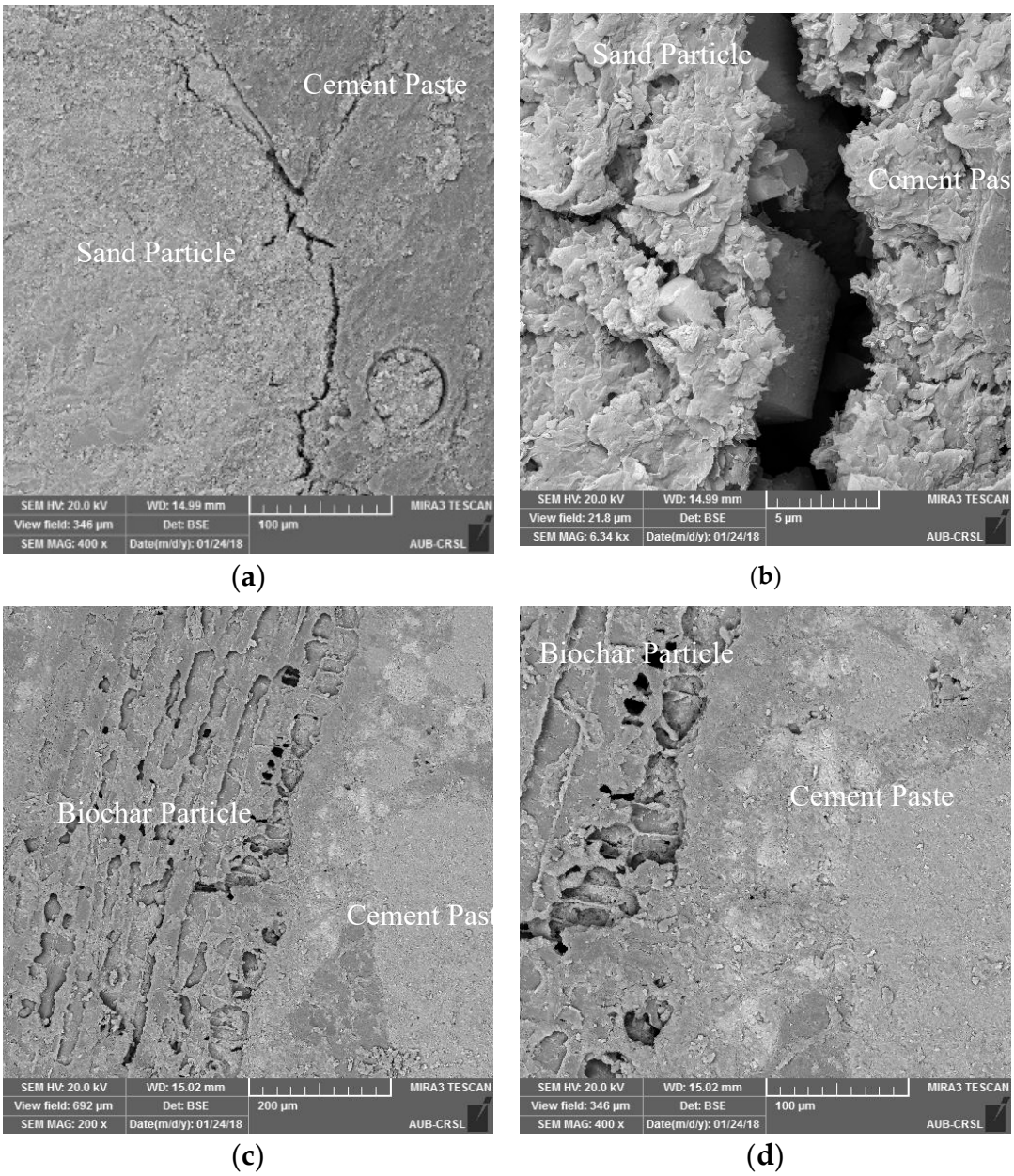

Figure 11. (**a**) Sand aggregate–cement paste interface at 400× magnification; (**b**) 6000× magnification showing complete detachment of the cement paste from the sand aggregate; (**c**) biochar aggregate–cement paste interface at 200× magnification; (**d**) 400× magnification showing the continuous interfacial transition zone (ITZ) and porous biochar particle.

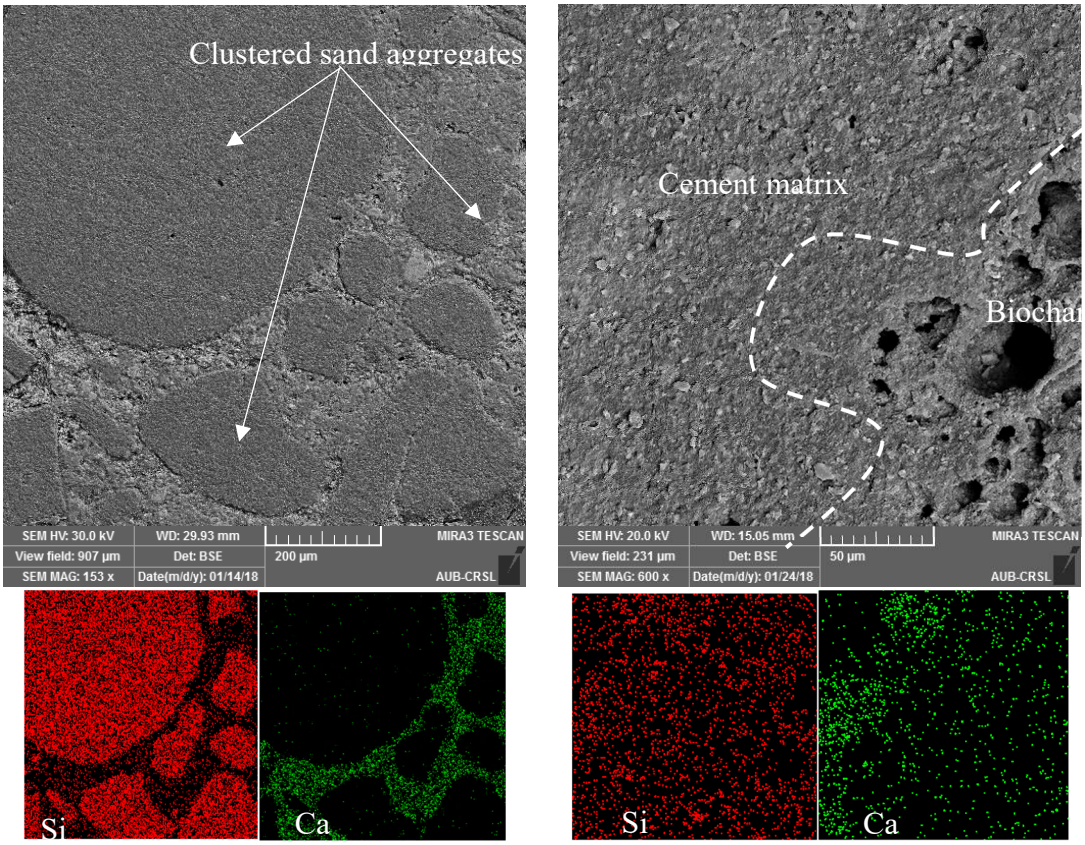

Figure 12. (**a**) SEM image of control sample (0% biochar) showing clustered sand aggregates and cement matrix at 150× magnification, with Si, Ca, and O X-ray maps; (**b**) SEM image of mortar mix at 600× magnification containing biochar with the X-ray maps.

Conversely, the detection of an ITZ around the outer rim of biochar particles seems difficult (Figure 11c,d). The mortar mix containing biochar is highly distinguished from the plain mix, due to the excessive concentrated pores and voids within the aggregates that are filled in with the cement paste. Microfractures are almost absent in this case. In Figure 12b, X-ray element maps show a complete dispersion of the elements Ca, Si, and O, without forming any belt or calcium hydroxide deposits along the outer rim of the biochar particles. In fact, the biochar and the cement matrix seem to be well linked and it is difficult to separate the two.

4. Conclusions

In this research, the use of biochar as a partial replacement of sand in cementitious mortar was experimentally investigated as a solution for the shortage of sand, while improving on the mechanical, physical, and microstructural properties of the bulk mortar. Upon extensive experimentation, the following conclusions and recommendations concerning some limitations of the research, which can be addressed in future studies, can be made:

- Biochar consists of interconnected fibers, forming a microporous cellular structure that can absorb and sustain a substantial amount of water to be used for internal curing. However, further studies on the effect of w/c ratio and the degree of saturation of biochar particles, prior to their inclusion in the mortar, is necessary to determine the optimum mix design that would yield a satisfactory mechanical and durable performance;

- The inclusion of partially saturated biochar in cementitious mortar composites generally decreases the compressive strength for various curing conditions. It is suggested that the biochar replacement of sand be limited to 15% and be fully saturated prior to inclusion in mortar for better results;
- It was found that the ITZ of biochar particles is superior to that of sand particles, due to the interlocking mechanisms exhibited by the pores at the face of the particles, which is caused by the water migrating from the internal reservoirs of the biochar to the surrounding paste. This migration promotes hydration reactions and results in a denser, less porous ITZ. However, quantitative analysis that quantifies the porosity, surface energy, and micro hardness of the interfacial transition zone at the biochar–cement paste interface should be carried out;
- Conducting further research to better understand and predict the effect of biochar inclusion on the durability of the mortars, including shrinkage deformation, is recommended.

Author Contributions: Conceptualization, R.M. and G.C.; methodology, R.M and G.C.; validation, R.M.; formal analysis, R.M. and G.C.; investigation, R.M.; resources, R.M.; data curation, R.M.; writing—original draft preparation, R.M. and G.C.; writing—review and editing, R.M. and G.C.; visualization, R.M.; supervision, G.C.; project administration, G.C.; funding acquisition, G.C.

Funding: This research was funded by the University Research Board at AUB.

Conflicts of Interest: The authors declare no conflict of interest. The funders had no role in the design of the study; in the collection, analyses, or interpretation of data; in the writing of the manuscript, or in the decision to publish the results.

References

1. Balasubramanian, J.; Gopal, E.; Periakaruppan, P. Strength and microstructure of mortar with sand substitutes. *Građevinar* **2016**, *68*, 29–37.
2. Manasseh, J. Use of crushed granite fine as replacement to river sand in concrete production. *Leonardo Electron. J. Pract. Technol.* **2010**, *17*, 85–96.
3. Modolo, R.; Ferreira, V.M.; Tarelho, L.A.; Labrincha, J.A.; Senff, L.; Silva, L. Mortar formulations with bottom ash from biomass combustion. *Constr. Build. Mater.* **2013**, *45*, 275–281. [CrossRef]
4. Andrade, L.; Rocha, J.; Cheriaf, M. Influence of coal bottom ash as fine aggregate on fresh properties of concrete. *Constr. Build. Mater.* **2009**, *23*, 609–614. [CrossRef]
5. Torkittikul, P.; Nochaiya, T.; Wongkeo, W.; Chaipanich, A. Utilization of coal bottom ash to improve thermal insulation of construction material. *J. Mater. Cycles Waste Manag.* **2017**, *19*, 305–317. [CrossRef]
6. Bilir, T.; Gencel, O.; Topcu, I.B. Properties of mortars with fly ash as fine aggregate. *Constr. Build. Mater.* **2015**, *93*, 782–789. [CrossRef]
7. Zhao, S.; Huang, B.; Shu, X.; Ye, P. Laboratory investigation of biochar-modified asphalt mixture. *Transp. Res. Rec. J. Transp. Res. Board* **2014**, *2445*, 56–63. [CrossRef]
8. Malkow, T. Novel and innovative pyrolysis and gasification technologies for energy efficient and environmentally sound MSW disposal. *Waste Manag.* **2004**, *24*, 53–79. [CrossRef]
9. Chen, D.; Yin, L.; Wang, H.; He, P. Reprint of: Pyrolysis technologies for municipal solid waste: A review. *Waste Manag.* **2015**, *37*, 116–136. [CrossRef]
10. Onyango, D.O. Pyrolysis: An alternative technology for municipal solid waste management. In Proceedings of the 2013 JKUAT Scientific Technological and Industrialization Conference, Nairobi, Kenya, 14–15 November 2013.
11. Lehmann, J.; Joseph, S. *Biochar for Environmental Management: Science, Technology and Implementation*; Routledge: Abingdon, UK, 2015.
12. Brewer, C.E. Biochar Characterization and Engineering. Ph.D. Thesis, Iowa State University, Ames, IA, USA, 2012.
13. Gupta, S.; Kua, H.W.; Low, C.Y. Use of biochar as carbon sequestering additive in cement mortar. *Cem. Concr. Compos.* **2018**, *87*, 110–129. [CrossRef]
14. Ali, A.; Sarmah, K. Novel biochar-concrete composites: Manufacturing, characterization and evaluation of the mechanical properties. *Sci. Total Environ.* **2018**, *616–617*, 408–416.

15. Famili, H.; Saryazdi, M.K.; Parhizkar, T. Internal curing of high strength self-consolidating concrete by saturated lightweight aggregate-effects on material properties. *Int. J. Civ. Eng.* **2012**, *10*, 210–221.
16. Henkensiefken, R.; Castro, J.; Kim, H.; Bentz, D.; Weiss, J. Internal curing improves concrete performance throughout its life. *Concr. InFocus* **2009**, *8*, 22–30.
17. Castro, J.; Keiser, L.; Golias, M.; Weiss, J. Absorption and desorption properties of fine lightweight aggregate for application to internally cured concrete mixtures. *Cem. Concr. Compos.* **2011**, *33*, 1001–1008. [CrossRef]
18. Henkensiefken, R.; Bentz, D.; Nantung, T.; Weiss, J. Volume change and cracking in internally cured mixtures made with saturated lightweight aggregate under sealed and unsealed conditions. *Cem. Concr. Compos.* **2009**, *31*, 427–437. [CrossRef]
19. Sun, X.; Zhang, B.; Dai, Q.; Yu, X. Investigation of internal curing effects on microstructure and permeability of interface transition zones in cement mortar with SEM imaging, transport simulation and hydration modeling techniques. *Constr. Build. Mater.* **2015**, *76*, 366–379. [CrossRef]
20. Lura, P.; Jensen, O.M.; Igarashi, S. Experimental observation of internal water curing of concrete. *Mater. Struct.* **2007**, *40*, 211–220. [CrossRef]
21. Bentz, D.P.; Stutzman, P.E. *Internal Curing and Microstructure of high-Performance Mortars*; ACI SP-256; Internal Curing of High-Performance Concretes: Laboratory and Field Experiences, American Concrete Institute: Farmington Hills, MI, USA, 2008; pp. 81–90.
22. Al-Khaiat, H.; Haque, M.N. Effect of initial curing on early strength and physical properties of a lightweight concrete. *Cem. Concr. Res.* **1998**, *28*, 859–866. [CrossRef]
23. Lam, H. Effects of Internal Curing Methods on Restrained Shrinkage and Permeability. Master's Thesis, University of Toronto, Toronto, ON, Canada, 2005.
24. Lura, P. Autogenous Deformation and Internal Curing of Concrete. 2003. Available online: http://resolver.tudelft.nl/uuid:1a1efc2d-a638-4787-b543-5bd643a39a4b (accessed on 23 March 2019).
25. Wong, H.S.; Buenfeld, N.R. Euclidean distance mapping for computing microstructural gradients at interfaces in composite materials. *Cem. Concr. Res.* **2006**, *36*, 1091–1097. [CrossRef]
26. Hilal, A.A. *Microstructure of Concrete. High Performance Concrete Technology and Applications*; InTech: Rijeka, Croatia, 2016.
27. Scrivener, K.L.; Crumbie, A.K.; Laugesen, P. The interfacial transition zone (ITZ) between cement paste and aggregate in concrete. *Interface Sci.* **2004**, *12*, 411–421. [CrossRef]
28. Vargas, P.; Restrepo-Baena, O.; Tobón, J.I. Microstructural analysis of interfacial transition zone (ITZ) and its impact on the compressive strength of lightweight concretes. *Constr. Build. Mater.* **2017**, *137*, 381–389. [CrossRef]
29. Lura, P.; Wyrzykowski, M.; Tang, C.; Lehmann, E. Internal curing with lightweight aggregate produced from biomass-derived waste. *Cem. Concr. Res.* **2014**, *59*, 24–33. [CrossRef]
30. Gupta, S.; Kua, H.W. Effect of water entrainment by pre-soaked biochar particles on strength and permeability of cement mortar. *Constr. Build. Mater.* **2018**, *159*, 107–125. [CrossRef]
31. EPA. *National Primary Drinking Water Regulations*. Available online: https://www.gvsu.edu/cms4/asset/E1327343-09F0-03FF-AA9032F47AD1EB9C/standards.pdf (accessed on 23 March 2019).
32. Bentz, D.P. Internal curing of high-performance blended cement mortars. *ACI Mater. J.* **2007**, *104*, 408.
33. Bentz, D.P. Influence of internal curing using lightweight aggregates on interfacial transition zone percolation and chloride ingress in mortars. *Cem. Concr. Compos.* **2009**, *31*, 285–289. [CrossRef]
34. Lo, Y.; Gao, X.F.; Jeary, A.P. Microstructure of pre-wetted aggregate on lightweight concrete. *Build. Environ.* **1999**, *34*, 759–764. [CrossRef]
35. Zhang, M.H.; Gjørv, O.E. Microstructure of the interfacial zone between lightweight aggregate and cement paste. *Cem. Concr. Res.* **1990**, *20*, 610–618. [CrossRef]